Available online at www.sciencedirect.com

ScienceDirect

Current Opinion in Structural Biology

Protein dynamics detected by magic-angle spinning relaxation dispersion NMR

Federico Napoli[1], Lea Marie Becker[1] and Paul Schanda

Abstract

Magic-angle spinning (MAS) nuclear magnetic resonance (NMR) is establishing itself as a powerful method for the characterization of protein dynamics at the atomic scale. We discuss here how $R_{1\rho}$ MAS relaxation dispersion NMR can explore microsecond-to-millisecond motions. Progress in instrumentation, isotope labeling, and pulse sequence design has paved the way for quantitative analyses of even rare structural fluctuations. In addition to isotropic chemical-shift fluctuations exploited in solution-state NMR relaxation dispersion experiments, MAS NMR has a wider arsenal of observables, allowing to see motions even if the exchanging states do not differ in their chemical shifts. We demonstrate the potential of the technique for probing motions in challenging large enzymes, membrane proteins, and protein assemblies.

Addresses

Institute of Science and Technology Austria, Am Campus 1, Klosterneuburg, 3400, Austria

Corresponding author: Schanda, Paul (paul.schanda@ist.ac.at)
(Napoli F.)
(Becker L.M.)
(Schanda P.)
[1] These authors contributed equally to this work.

Current Opinion in Structural Biology 2023, **82**:102660

This review comes from a themed issue on **Biophysical Methods (2023)**

Edited by **Irina Gutsche** and **Gaetano T. Montelione**

For complete overview of the section, please refer the article collection - Biophysical Methods (2023)

Available online 1 August 2023

https://doi.org/10.1016/j.sbi.2023.102660

Keywords:

Nuclear spin relaxation, Near-rotary-resonance relaxation dispersion, Rocking motion, Loop motion, Side-chain rotamer transitions, Solid-state NMR.

Dynamic structural biology

Biological processes are determined by the way how proteins interact with each other in the complex cellular environment and how the jiggling and wiggling of atoms enable enzymatic catalysis, recognition, binding, and folding. Despite the enormous usefulness of the static structures determined from proteins frozen in crystals or on EM grids, it is of great importance to include dynamics for deciphering how biomolecules function.

Nuclear magnetic resonance (NMR) spectroscopy occupies an important place in studies of protein dynamics because it can determine equilibrium dynamics with a resolution of individual atoms, without the need for crystallization or freezing and without adding any chemical labels. Because NMR exploits a property inherent to every atom (^{1}H, ^{13}C, ^{15}N, ^{31}P), it simultaneously probes the local environment at hundreds of sites. Nuclear spins not only report on their average environment, but they are exquisitely sensitive to the way the environment fluctuates around the time-averaged conformations.

Solution-state NMR spectroscopy is routinely used for the determination of structures and dynamics of proteins below ca. 40 kDa. Due to the overall molecular tumbling in solution, some interactions that a nuclear spin has with its environment are averaged to zero, which makes spectra simple; but if the overall tumbling is slow (tens of nanoseconds or longer, corresponding to proteins of ca. 40 kDa or more), then it entails rapid spin relaxation, i.e. a loss of signal. Consequently, studying larger proteins becomes tricky. Solution-state methyl-TROSY NMR can provide powerful insights into motion and function [1,2], but it reduces the number of reporters to methyl groups only.

Many molecular assemblies of biological interest are inherently insoluble (e.g., membrane proteins, amyloid fibrils), excluding solution-state NMR. Even for inherently soluble large proteins, which are difficult to study by solution-state NMR because of the aforementioned slow tumbling, one may want to have those proteins in an immobilized state (e.g., sedimented). All these cases, where the protein molecules are not tumbling, are herein referred to as a solid state; besides insoluble assemblies (large capsids, tubes, fibrils) or proteins embedded in liposomes, bound to cell walls, or embedded in some matrix or in a crystal, one may obtain "solid" samples also by ultracentrifuging a solution of protein to obtain a pellet, which has the properties of a solid [3,4]. Typical samples for solid-state NMR are highly hydrated

(typically more than 50% of the sample mass is water), and the historical term "solid" might be misleading.

As the molecules in solid-state NMR samples are fixed in orientation, the aforementioned averaging of interactions of a spin with its environment, which is brought about by overall tumbling in solution, is absent. Because of these large, orientation-dependent interactions, NMR spectra of solids, i.e., a static collection of molecules oriented in all possible directions, are very complex and hardly useful. In order to obtain spectral resolution allowing to resolve individual atoms, one needs to mimic the overall tumbling process by subjecting the entire sample to rapid rotation around the so-called magic angle (ca. 54.7°, which is the zero-crossing of a mathematical function that describes the orientation-dependence of the interactions). Sample-spinning frequencies range up to ca. 160 kHz nowadays. In contrast to the stochastic tumbling in solution, the sample rotation subjects the spin interactions to a well-defined time dependency. The spectroscopist can use pulses of electromagnetic field in the radio-frequency range (RF pulses) to rotate spins and thereby create interferences between the time-dependent sample rotation and the time-dependent rotation of spins by the pulses. This opens a vast playground for the spectroscopists to design RF pulse sequences tailored to detect a particular aspect of the molecular structure or dynamics, with more possibilities than what solution-state NMR can offer.

This review focuses on such magic-angle spinning (MAS) NMR experiments and more specifically on MAS NMR spin-relaxation experiments suitable to probe motions on the nanosecond-microsecond-millisecond (ns–μs–ms) timescales. The reader is referred to other reviews on MAS NMR dynamics measurements for a more in-depth view [5–10].

How NMR observables can see molecular motion

Dynamics of a molecule—irrespective of whether it is local bond libration or large-scale domain motions—reorients atoms and bonds in space. Therefore, it modifies the spatial distribution of electrons (molecular orbitals), and many interatomic distances and orientations. Figure 1 illustrates a simple example of rotation of a phenylalanine ring around its χ_2 angle. As the ring flips between the two equivalent states, the orientation of the indicated C–H bond is flipped by 120°; moreover, the C–H site experiences different environments in the two states, e.g., because more or less electronegative neighbors render the two environments nonequivalent. For a ring buried in the interior of a protein, this transition is associated with a significant energy barrier, and flips often take many μs or longer [11]. Within each well, the ring undergoes faster, smaller-angle rotations (Figure 1b).

From an NMR standpoint, these fluctuations of bond angles, distances, and electronic environments translate to fluctuations of spin interactions: (i) The electronic environment gives rise to a local magnetic field at the location of the nucleus, which partially shields the external magnetic field. This so-called chemical-shift interaction essentially reflects how the electrons are distributed around the nucleus; in general, this distribution is different in different directions around a nucleus, i.e., anisotropic. The orientation-averaged value of the chemical shift, also called the isotropic chemical

Figure 1

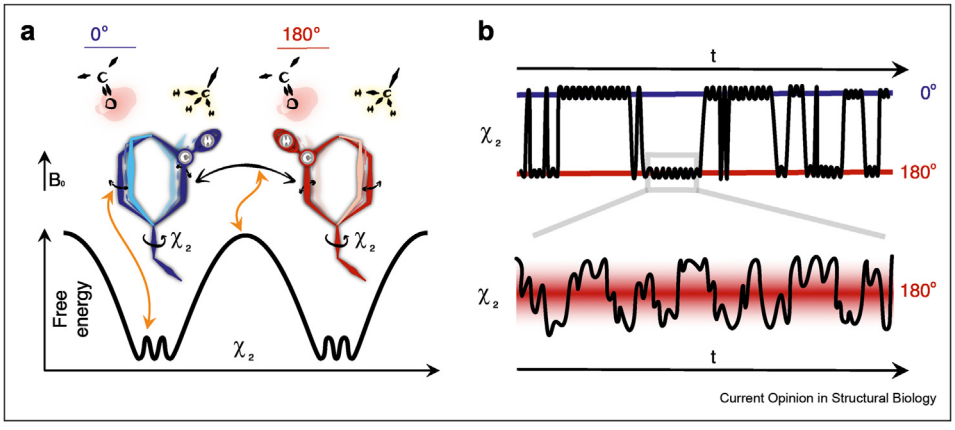

Motion probed by MAS NMR, as exemplified by ring flips. (a) Energy landscape of a phenylalanine ring embedded in a protein. The ring can adopt two main conformations (red and blue), separated by a 180° flip of the aromatic ring, and additional faster small-scale rotations within each well. In the two states, the highlighted C–H site is subjected to different electronic environments and interatomic distances. Additionally, the orientations of the bond and the chemical-shielding tensor (depicted by an ellipsoid), relative to the static magnetic field, are altered. **(b)** Time trace of the χ_2 dihedral angle slow ring flip motion (top) and fast low-amplitude rotation. These faster motions can be studied by, e.g., longitudinal relaxation (R_1, see Figure 2h).

shift, determines the position of a given resonance peak in an NMR spectrum. As the molecule undergoes some conformational change (e.g., changes of dihedral angles or distances from the atom to others), so does the electronic cloud, and therefore, the isotropic chemical shift fluctuates stochastically. As a consequence, the spin experiences a local fluctuating magnetic field due to dynamics.

(ii) Moreover, the chemical shift is generally anisotropic, i.e., the shielding is different along different spatial directions. The instantaneous resonance frequency of a given spin depends on the orientation of this chemical-shift anisotropy (CSA) tensor with respect to the magnetic field. Motion means that the spin experiences a fluctuation of its CSA tensor.

(iii) Besides the chemical shift, the other very important interaction is the dipolar coupling which is a through-space interaction between two spins. It depends on the distance between nuclei, and the angle between the inter-atomic vector and the magnetic field. Thus, like the anisotropic part of the chemical-shift interaction discussed previously, the dipolar coupling is also orientation-dependent. Again, molecular motion leads to a fluctuation of the dipolar coupling, which translates to a fluctuating magnetic field, from the spin's standpoint.

For completeness, two other interactions shall not be left out in this discussion: firstly, the quadrupolar coupling, which is the interaction of the quadrupole moment of the nucleus with the electric-field gradient. Because ^{1}H, ^{13}C, and ^{15}N nuclei do not possess a quadrupole moment, these nuclei are not concerned. Relevant for biomolecules, however, are deuterium (^{2}H) nuclei, and we refer the reader to interesting developments of using deuterium for detecting slow motions in proteins [12]. In the remainder of this review, we will focus only on spins without quadrupole moment. Lastly, the spins also have a through-bond coupling, which for simplicity we leave out here, as it generally has a minor role for dynamics studies.

To come back to the example of Figure 1, a ring flip entails a change of the couplings, e.g., that of the ^{1}H spin with the bonded ^{13}C spin or with the surrounding ^{1}H spins; moreover, the orientation of the chemical-shielding tensor (indicated as an ellipse) in space is altered; and lastly, the fact that the ^{1}H spin is located in a different chemical environment also means that its isotropic chemical shift is different in the two conformations.

Spins are sensitive to the amplitude and time scale of these fluctuations, i.e., (i) the (orientationally averaged, i.e., isotropic) chemical shift, (ii) the CSA, and (iii) the dipolar couplings, in two ways.

On one hand, the time-averaged interaction strength, compared to its expected value in the absence of motion, directly reports on the amplitude of motion, averaged over all time scales shorter than a few tens of μs. In solids, this reduction of the interaction strength reports on internal motional amplitudes. (More precisely, it is the product of the relative populations of states and a function describing the difference in the orientation between those, which determine the amount by which the dipolar coupling is reduced.)

On the other hand, the speed of relaxation of a spin towards its thermal equilibrium, after it has been excited by RF pulses, depends on the amplitudes and timescales of these fluctuations. Again, solid-state NMR has an inherent advantage over its solution-state counterpart for detecting motions on timescales longer than tens of nanoseconds, even in the absence of isotropic chemical-shift differences. This is because in solution, only the isotropic chemical-shift fluctuations survive as reporters of slow motion, whereas CSAs and dipolar couplings are averaged to zero by the tumbling. Several MAS NMR approaches are available for detecting μs−ms motions in MAS NMR, including Carr−Purcell−Meiboom−Gill relaxation dispersion [13], chemical-exchange saturation transfer [14], centerband-only detection of exchange [15,16], differential multiple-quantum relaxation [13], or deuterium line shape analysis [17]. We refer the interested reader to additional reviews on topics of dynamics by MAS NMR [18,6,19−21]. The focus of this review is on a technique that has proven particularly versatile and robust for detecting μs−ms motion: $R_{1\rho}$ relaxation dispersion (RD) experiments.

NMR relaxation experiments workflow and its information content

A relaxation measurement generally consists of preparing a particular spin state by RF pulses, and following its evolution during a relaxation delay by measuring the peak intensity remaining at the end of the relaxation delay. By repeating the measurement, and increasing the relaxation delay from one experiment to the next, one obtains the relaxation-rate constant from fitting this intensity decay as a function of the relaxation delay length, most often using an exponential decay. To obtain site-specific information, the readout is often a two-dimensional correlation spectrum that separates, e.g., all amide signals according to the ^{1}H and ^{15}N frequencies. For the case of $R_{1\rho}$ measurements (Figure 2a,b), a spin state is prepared and allowed to relax during a time t_{relax} in the presence of a continuous RF pulse (called spinlock pulse) with a certain RF field strength ν_{SL} (in kHz).

In $R_{1\rho}$ RD measurements, the experiment is repeated with different ν_{SL} values, and the dependency of $R_{1\rho}$ on ν_{SL} is called relaxation dispersion (Figure 2b−d). μs−ms

Figure 2

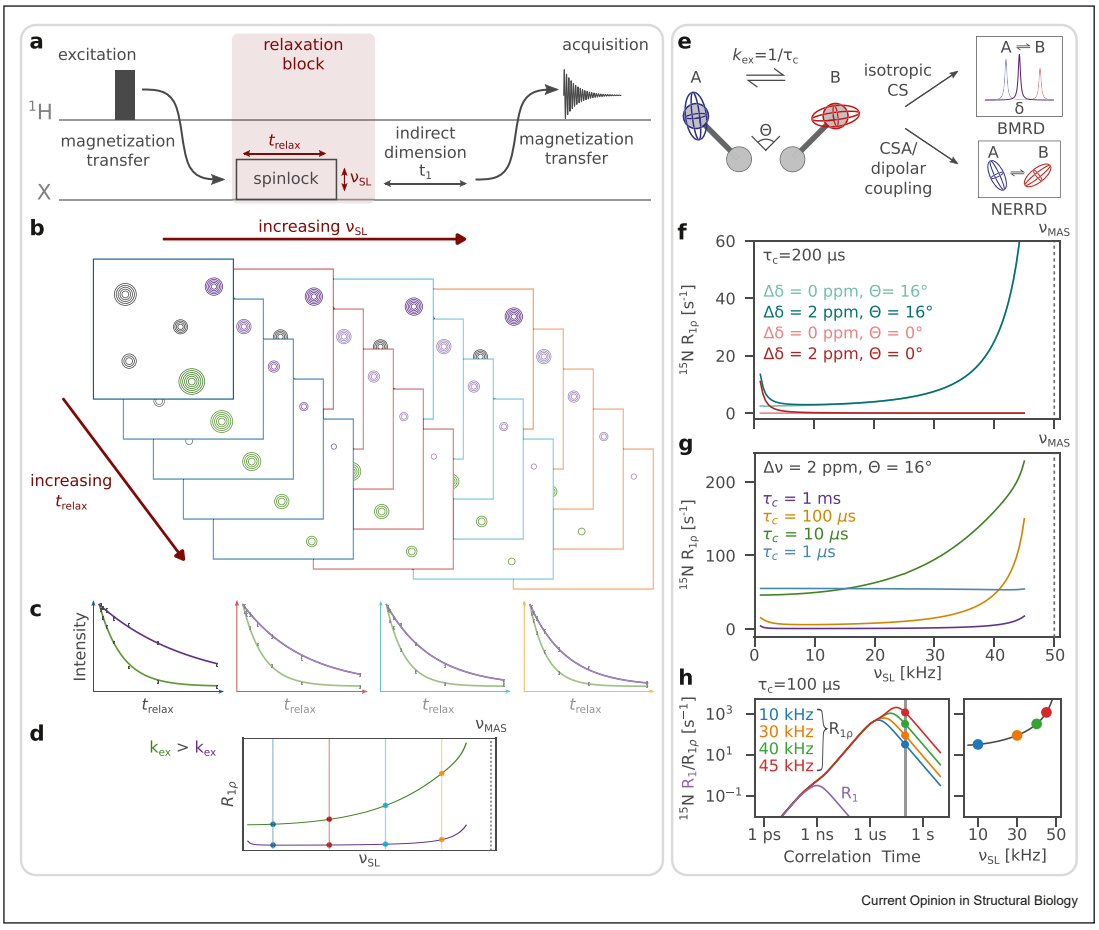

***$R_{1\rho}$* relaxation dispersion measurements in MAS NMR. (a)** Schematic depiction of a two-dimensional pulse sequence to measure $R_{1\rho}$ relaxation. After excitation of protons, magnetization is transferred to the nucleus of which the relaxation properties are measured (e.g ,^{15}N or ^{13}C). In the relaxation block, an RF spinlock pulse of variable length t_{relax} and field strength ν_{SL} is applied. Then, the two chemical-shift frequencies are recorded to obtain amino-acid wise resolution. **(b)** A single $R_{1\rho}$ rate constant is obtained by recording a series of experiments with increasing t_{relax} and monitoring the t_{relax}-dependent intensity decay. A relaxation dispersion profile is recorded by repeating measurements with increasing ν_{SL}. **(c)** The extracted peak intensities are fitted to exponential decays to determine the relaxation-rate constant at each ν_{SL}. **(d)** The resulting relaxation dispersion profile **(e)** A simple two-site model of a two-spin system (e.g., ^{1}H–^{13}C), involving rotation of the bond by an angle Θ at an exchange-rate constant k_{ex}. Motions results in (i) fluctuations of the isotropic chemical shift δ of one nucleus or (ii) reorientation of anisotropic-spin interactions (chemical-shift anisotropy and dipolar coupling), which are depicted here by an interaction tensor (ellipsoid). **(f)** Spin simulations of this jump model with a correlation time τ_c of 200 µs and different combinations of Δδ and Θ. A change of δ leads to Bloch–McConell relaxation dispersion at low ν_{SL}, whereas reorientational jumps (Θ) result in near-rotary-resonance relaxation dispersion as ν_{SL} approaches ν_{MAS}. **(g)** Dependence of $R_{1\rho}$ on the correlation time τ_c. **(h)** Different view of the same situation, plotted as a function of τ_c, highlighting that $R_{1\rho}$ near-rotary-resonance relaxation dispersion occurs only for µs–ms motion.

fluctuation of the isotropic chemical shift results in a population-weighted averaged peak position; it induces line broadening and an increase of $R_{1\rho}$ at low RF field strengths. This latter effect is termed Bloch–McConnell relaxation dispersion (BMRD) and is also present in solution NMR.

In the vicinity of so-called rotary-resonance conditions ($\nu_{SL} = \frac{1}{2}\nu_{MAS}$, $\nu_{SL} = \nu_{MAS}$, $\nu_{SL} = 2\nu_{MAS}$), on the other hand, interference effects between ν_{SL} and the magic-angle sample spinning frequency ν_{MAS} lead to enhanced $R_{1\rho}$. At these resonance conditions, the periodic fluctuation of the dipolar interaction that is imposed onto, e.g., a pair of ^{1}H–^{13}C atoms by MAS is "undone" by the periodicity imposed onto the spins by the RF field. As a consequence, the MAS-induced averaging of the dipolar coupling (which leads to sharp lines) is counteracted for the time during which the RF field is on. This effect, called recoupling, is used in experiments that exploit the dipolar coupling, e.g., for correlating frequencies of spins, where, e.g., the ^{13}C coherence is transferred to ^{1}H (and thereby, it decays quickly). This effect is present even in samples without any dynamics.

However, in the presence of dynamics, this decay of coherence occurs not only exactly at the resonance conditions, but also around them, i.e., the resonance conditions are broadened by dynamics, which appears as an increased relaxation. This broadening of the resonance conditions (i.e., an increase in $R_{1\rho}$; Figure 2d,f,g) happens only if this stochastic motion is of the order of the sum or difference between the sample rotation (MAS) and spin rotation (RF field) frequencies.

At the different conditions mentioned previously, different types of interactions are relevant. For example, at $\nu_{SL} = \frac{1}{2}\nu_{MAS}$ it is the quadrupolar coupling (if applicable) and the homonuclear dipolar coupling, such as between two ^{1}H spins, which get "recoupled" and give rise to the enhanced relaxation. At $\nu_{SL} = \nu_{MAS}$, it is the heteronuclear dipolar coupling and the CSA. Thus, at the latter condition, one sees motion of , e.g., the ^{1}H$-^{15}$N bond and the ^{15}N CSA, whereas at the former condition, one sees the relative motion of two ^{1}H spins.

This effect of enhanced relaxation when the RF field and MAS frequencies approach these specific conditions is also called near-rotary-resonance relaxation dispersion (NERRD), a term introduced by Kurauskas et al. [22]. It is specific to MAS NMR and is a useful detector of the presence of µs motions, as demonstrated by example calculations and spin dynamics simulations (Figure 2g–h).

Accurate quantification of $R_{1\rho}$-rate constants is challenged by the fact that the apparent decay rate constant is not only caused by dynamics, but also by unwanted effects unrelated to dynamics, which may lead to faster decay. Particularly, this is the case for so-called dipolar dephasing, which arises due to the presence of strong dipolar ^{1}H$-^{1}$H couplings that are not sufficiently well-suppressed by MAS. Faster MAS [23] and the replacement of non-needed ^{1}H nuclei by ^{2}H (which has weaker dipolar couplings) help suppressing these unwanted effects. In this respect, an important development is the selective introduction of sparse protonation in an otherwise deuterated environment, leaving ^{1}H only at the sites one wants to detect. As higher MAS frequencies (currently up to ca. 160 kHz) and specific labeling of side chains became available, RD experiments are becoming increasingly popular and widespread.

From MAS NMR RD data to motional models

Different approaches can be used to interpret relaxation data and characterize the underlying motion [9]. As NMR parameters probe the motion only indirectly, their interpretation generally involves models.

Explicit physical models may be adapted whenever one knows about possible motions of a molecule. This is particularly the case for, e.g., ring flip motion (symmetric two-site jump) or other side-chain rotamer transitions (asymmetric n-site jumps). Two-state models are often also used for interpreting BMRD data, e.g., an exchange between a major and a minor conformer. Further physical models are, e.g., rocking motion of a protein or a protein domain within a crystal [22] or a complex [24] or of a helix in a membrane [25]. These models are ideally backed up by molecular dynamics simulations. Explicit physical models are also used for treating (mostly faster) local librations (e.g., assuming the wobbling of a bond in a cone).

Other classes of models make assumptions about the mathematical form of the correlation functions, rather than assuming an explicit physical motional model [26–30]. For example, Smith et al. proposed an approach that aims to reflect the complexity of molecular motion by extracting the amplitude of motion in different timescale windows, the so-called "detectors" [31,32], from relaxation data and (optionally) dipolar order parameters (but not BMRD data). The idea of the detectors approach is the realisation that different relaxation experiments (e.g., longitudinal relaxation at different magnetic field strengths or transverse relaxation recorded with different strengths of applied radio-frequency fields) are sensitive to different timescales of motion. Therefore, given a set of experimental data, collected under certain conditions, the approach searches to find which time windows the experimental data can report on and determines the "amount of motion" (amplitude) in each of these time windows, aiming to reflect the multitude of motions occurring at different time scales. It makes fewer assumptions than, e.g., an explicit two-site exchange model that is often used to analyze BMRD data; one may argue that the result of the detectors approach may be more reliable if one does not know whether a certain models is actually justified. It allows for a combined analysis of different experiments aiming to draw an extensive picture of the complexity of molecular motion and also link them to molecular dynamics simulations [33,34].

Applications

Protein motion occurs on various timescales. In some cases, the mobility of individual side chains holds the key to function of enzymes. Often, larger segments of the protein, such as long loops or entire secondary-structure elements, sample different conformational states. In the following, we provide some spotlights on recent RD studies, from local to long-range motions.

Side-chain dynamics

Established originally for solution-state NMR [2], methyl-labeling in deuterated proteins has turned out very useful for MAS NMR. $^{13}CHD_2$-labeling in deuterated proteins has been used to study sub-µs rotamer equilibria [35,36] and also for NERRD

experiments of Ile, Leu, and Val side chains in the 0.5-MDa large TET2 aminopeptidase complex [37]. Selective labeling methods are being extended to other residues, such as aromatics [38]. These are over-represented at protein interfaces and catalytic sites and can report on local unfolding events (so-called breathing motion) if ring-flip events are observed [39]. Selective labeling of phenylalanines with $^{1}H-^{13}C$ labels in either the site that is colinear with the ring axis (C^{ζ}) or is inclined by 60° to the axis (C^{ε}) was introduced in the dodecameric TET2 peptidase [40]. These two labeling schemes have allowed the detection of the timescale of ring flips and ring-axis motion. Ring flips of buried aromatics require larger-scale breathing motions of proteins that create a transient void volume to allow for the flip. Interestingly, the timescales of flips of the ten Phe residues in TET2 vary greatly, from few ns to hundreds of μs, and MD simulations have been used to rationalise the findings [40]. Moreover, experiments down to −173 °C allowed studying the thermal activation of the fast ring-flip motion. Using BMRD experiments, localized μs−ms dynamics was also detected at the protomer interfaces and on the structural pathway between the entry pore and the catalytic site.

The same Phe-labeling scheme has been used to probe how the crystalline environment impacts aromatic ring flips by comparing three different crystal forms of ubiquitin, using ^{13}C and ^{1}H $R_{1\rho}$ data and MD simulations [41]. Using phenylalanine and tyrosine-labeling of two amyloid fibrils (HET-s and HELLF), we have recently revealed that the amyloid core is rigid, without any ring flips up to at least hundreds of milliseconds (presumably longer), whereas rings on the surface rotate on a μs timescale [42]. The backbone dynamics of the HELLF fibrils have also been studied in a very rigorous study by Smith, Ernst et al. [43]. Note that solution NMR is unable to quantify motions on the ns−μs timescale, such that ring-flip motion is often hard to quantify. Overall, the use of selectively labeled amino acids with MAS NMR has revealed a surprisingly diverse spectrum of motion.

The Pintacuda lab has studied how metal-binding to the active site of superoxide dismutase alters the side-chain dynamics (using ^{15}N-labeled histidine sites) and backbone dynamics [44]. Metal-binding does not simply rigidify the protein but rather redistributes the timescales on which motions occur.

Motion of secondary structure elements

Frequently, conformational exchange associated with protein function involves several residues, in a catalytic pocket or throughout a loop, α-helix or β-sheet. This is the case for an intramembrane rhomboid protease, GlpG, which was studied in liposomes [45] (Figure 3a). BMRD data demonstrated how one of the transmembrane helices of GlpG undergoes a transition between a closed, major state and an open, minor state. Fitting of the dispersion curves to a global, two-state exchange model revealed a motional timescale of ca. 40 μs. Conformational dynamics has also been studied in, e.g., rhodopsin, providing evidence for collective motions of transmembrane helices [25].

Figure 3

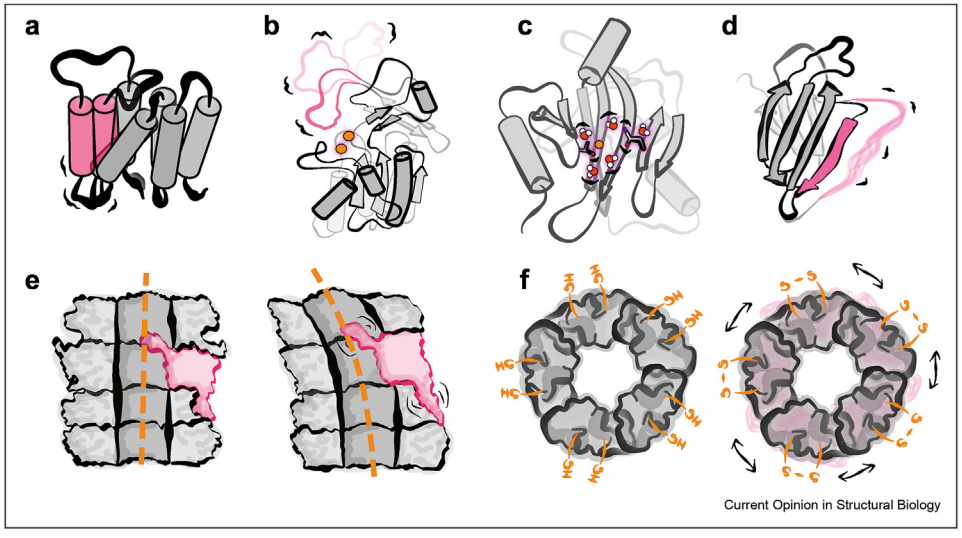

Examples of protein motion investigated by solid-state NMR. (a) Loop and helix dynamics in an intramembrane protease studied in liposomes [45]. **(b)** Motion of a flexible loop, involved in the stabilization of substrate in the active site of the TET2 aminopeptidase [37]. **(c)** Shared motion of a protein−water network at the active site of hCAII [47]. **(d)** Transient unfolding of a β-sheet in the excited state of a microglobulin mutant, responsible for its increased aggregation propensity [50]. **(e)** Bacteriophage tail tube−bending mediated by flexible hinge regions [53]. **(f)** Dynamic disorder induced by disulfide-bonding in a decameric peroxiredoxin [56].

The power of MAS NMR to study large molecular assemblies has allowed elucidating the role of a highly flexible loop in TET2 aminopeptidase, using $^{13}CHD_2$ methyl-directed NERRD experiments mentioned previously [37]. A long loop in the catalytic chamber, which could not be resolved in X-ray crystallography structures, undergoes μs motions and can adopt conformations that stabilize the substrate at the active site (Figure 3b). The flexibility allows substrate passage, while also retaining the ability to stabilize the substrate once bound to the catalytic center. Loop dynamics on the μs time scale have also been identified in SH3 crystals, using ^{1}H and ^{15}N $R_{1\rho}$ methods [46].

Singh, Linser et al. identified the presence of protein−water network-shared motion in the catalytic site of the 29-kDa large human carbonic anhydrase hCAII (Figure 3c). By combining ^{15}N $R_{1\rho}$ BMRD with ^{1}H and ^{15}N $R_{1\rho}$ NERRD profiles, they observed unambiguous dynamics of the water−H−bonded moieties, which was severely decreased after binding of the inhibitor dorzolamide. Comparing these results with the knowledge about ordered protein−water networks from X-ray crystallography, they proposed that water in the catalytic pocket not only acts as a solvent, but its structural role might determine the dynamic personality of the enzyme [47].

Occasionally, changes in dynamics are the determinants behind the phenotypical differences in protein mutants. Several point mutants of the KcsA potassium channel were investigated, mimicking substitutions present in the eukaryotic voltage-gated channels [48,49]. The mutants, characterized by different gating modes, showed severe shifts in dynamics at the selectivity filter, the entry access for potassium ions.

Mutations are sometimes responsible for disease, such as, for example, amyloidosis. The effect of the highly pathogenic D76N mutation in β2-microglobulin was elucidated by solid-state NMR in crystals [50]. This causes the weakening of a set of electrostatic interactions, determining the loss of structure in the protective edge β-strand (Figure 3d). The highly aggregation-prone regions are therefore exposed, triggering amyloid formation.

Besides probing the function-related motion, MAS NMR experiments have also allowed addressing how the crystalline environment impacts motion. In ubiquitin, a peptide plane in a β-turn flips between two conformations, including some side-chain and hydrogen-bonding rearrangements. It was shown that the process, which had been extensively characterized in solution, is still present in crystals, although the exchange kinetics can become slowed down by an order of magnitude. Moreover, the predominant state in one crystal can become a minor state in another [51,52].

Motions involving larger structural elements

Solid-state NMR is particularly powerful for large protein complexes or assemblies. Zinke et al. analyzed ^{15}N R_1 and ^{15}N $R_{1\rho}$ rate constants in polymerized tail tubes of the bacteriophage SPP1 (Figure 3e). They identified highly dynamic hinge regions, undergoing stretching motion upon tube bending. Flexibility was confirmed by the pronounced density variances of these regions in the cryo-EM maps. Furthermore, BMRD was measured to detect motion on the μs−ms timescale. Most residues in the barrel, forming the vertebrae of the tube, were involved in slow motion, and the $R_{1\rho}$ values could be fitted in a correlated manner to a two-state exchange model. Thus, this was proposed to represent tube bending [53].

The overall motion of an entire protein within its environment has also been reported for several small proteins. The Lewandowski group has revealed by $R_{1\rho}$ experiments that the protein GB1 has small-amplitude overall motion when it is bound to an antibody, while it is more fixed within the crystal [24]. RD measurements, backed up with MD simulations and crystallography, have revealed that ubiquitin has markedly different overall rocking motion within different crystal lattices [54,22]. Krushelnitsky et al. have investigated rocking motion also in crystals of GB1 and SH3 [55]. These findings provide important insights into overall motion and its relationship to crystallographic resolution and its modeling (B-factors, translation-libration-screw modeling of crystal structures, etc); unlike crystallography, MAS NMR is also able to quantify the time scale of overall motions.

A recent study [56] has used MAS NMR RD experiments to investigate the effects of disulfide-bond formation on the dynamics and structure of the peroxiredoxin Tsa1, an important player for detoxifying cells from peroxides, that forms 220-kDa large decameric rings (Figure 3f). Its functional cycle involves the formation of a disulfide bond. Disulfide-bond formation induces μs motion, particularly around the two involved cysteines, which are sensed by ^{15}N $R_{1\rho}$ NERRD data of amides throughout almost the entire protein. Interestingly, a large part of the protein in its disulfide-bonded state had been unobservable by crystallographic methods, presumably due to the dynamics that MAS NMR has identified. The dynamics has been ascribed to structural frustration, i.e., the inability to simultaneously satisfy favorable interactions, due to the constraints imposed by the disulfide. In addition, BMRD data have revealed dynamics at the intersubunit interfaces of the decameric rings, in both the reduced and oxidised states.

Outlook

Over the last 10 years, MAS NMR has made a substantial leap from small crystalline model proteins to dynamics investigations of, e.g., membrane proteins and enzymes of hundreds of kilodaltons in total size, and monomer sizes of several hundred residues. The examples cited previously provide a glimpse of the types of insight that one can obtain from such data. This information is highly complementary to the structures obtained by crystallography or cryo-EM, and several examples show that often the interesting dynamic parts are simply unobservable in crystallographic and EM models.

The continuous improvement of NMR hardware (in particular faster MAS), isotope-labeling and pulse-sequence methods has been (and will continue to be) of great importance. For example, MAS frequencies of 50 kHz and above, combined sparse protonation in a deuterated background and ^{1}H-detected pulse sequences, have been instrumental to allow for artefact-free relaxation dispersion measurements. MD simulations have been extremely useful for interpreting the NMR data and providing atom-level details that experimental techniques have a hard time to get. We foresee further developments in all these areas:

(i) The need for deuteration-specific labeling may be relaxed to some degree with even faster MAS (soon towards 200 kHz).

(ii) On the other hand, using organic chemistry to design new selectively ^{1}H−^{13}C−^{1}H−^{15}N−^{19}F-labeled side chains holds the key to focusing on dynamics of sites that currently are not so easy to study at the same level of detail as the ones described previously. It will be exciting to be able to dwell on particular sites of, e.g., enzymes and decipher the motions of, e.g., Ser, Glu, or His side chains often found in the active sites of enzymes.

(iii) On the pulse sequence design side, we are developing methods that make RD experiments more sensitive. In particular, we are exploring methods to decouple ^{1}H spins, which would enhance sensitivity particularly close to the rotary-resonance conditions (where oscillations at the onset of the spinlock severely reduce sensitivity [55]), and which would also allow extending the methods towards slower (ms) motions. Ongoing work establishes the potential of the method. While writing this review, an interesting work along these lines has been published too [57].

(iv) The addition of paramagnetic cosolutes can accelerate data acquisition in NMR by speeding up longitudinal relaxation between repetitions of scans, thereby allowing to repeat experiments faster [58−60]. That this would work for quantifying relaxation in dynamics measurements is not granted, as the paramagnetic cosolute enhances the relaxation in a way that is not related to the dynamics of interest; one may, however, either fit both the dynamics part and the paramagnetic part (related to solvent accessibility) simultaneously to the relaxation data or assume (and verify) that the paramagnetic contribution is independent of the applied RF field and thus analyze a the RF-field dependency (i.e., relaxation dispersion) only in terms of µs motion, as pioneered by Lewandowski and co-workers for BMRD experiments [61]. Alternative approaches to $R_{1\rho}$ RD experiments for detecting µs−ms motions, such as Carr−Purcell−Meiboom−Gill and differential multiple-quantum relaxation [13] are also promising.

(v) An obvious further development is towards other nuclei, such as ^{19}F. Although ambitious, it would be exciting to push methods that detect µs motions not only by "local" spies but also by directly monitoring the fluctuation of long-range interatomic distances.

(vi) The way how data are analyzed has made progress from simple "model-free" treatments a decade ago to more advanced methods such as the detectors approach. A very exciting development along these lines is the direct incorporation of MD simulations into the data fitting, as pioneered by Smith et al. [9,34]. A challenge for the analysis of µs motions using methods such a MAS NMR RD/MD analysis is that for statistically relevant sampling, one requires MD data equivalent to many tens of µs. These challenges are being worked on extensively [62−64]. Moreover, developments of MD integration data with experimental methods [65] will likely be instrumental also for MAS NMR.

CRediT author statement

F. Napoli: Conceptualization, writing, visualization (Figures 1 and 3). L. M. Becker: Conceptualization, writing, visualization (Figure 2). P. Schanda: Conceptualization, writing.

Declaration of competing interest

The authors declare that they have no known competing financial interests or personal relationships that could have appeared to influence the work reported in this paper.

Data availability

No data was used for the research described in the article.

Acknowledgements

We thank Petra Rovó for critical reading of this manuscript. We acknowledge the Austrian Science Foundation FWF (project AlloSpace, number I5812−B) and funding by the Institute of Science and Technology Austria.

References

Papers of particular interest, published within the period of review, have been highlighted as:

* of special interest
** of outstanding interest

1. Rosenzweig R, Kay LE: **Bringing dynamic molecular machines into focus by methyl-TROSY NMR**. *Annu Rev Biochem* 2014, **83**:291–315.
2. Sheppard D, Sprangers R, Tugarinov V: **Experimental approaches for NMR studies of side-chain dynamics in high-molecular-weight proteins**. *Prog Nucl Magn Reson Spectrosc* 2010, **56**:1–45.
3. Mainz A, Jehle S, Van Rossum BJ, Oschkinat H, Reif B: **Large protein complexes with extreme rotational correlation times investigated in solution by magic-angle-spinning NMR spectroscopy**. *J Am Chem Soc* 2009, **131**:15968–15969.
4. Bertini I, Luchinat C, Parigi G, Ravera E, Reif B, Turano P: **Solid-state NMR of proteins sedimented by ultracentrifugation**. *Proc Natl Acad Sci USA* 2011, **108**:10396–10399.
5. Rovo P: **Recent advances in solid-state relaxation dispersion techniques**. *Solid State Nucl Magn Reson* 2020, **108**, 101665.
6. Schanda P, Ernst M: **Studying dynamics by magic-angle spinning solid-state nmr spectroscopy: principles and applications to biomolecules**. *Prog Nucl Magn Reson Spectrosc* 2016, **96**:1–46.
7. Lewandowski JR: **Advances in solid-state relaxation methodology for probing site-specific protein dynamics**. *Acc Chem Res* 2013, **46**:2018–2027.
8. Linser R, Sarkar R, Krushelnitzky A, Mainz A, Reif B: **Dynamics in the solid-state: perspectives for the investigation of amyloid aggregates, membrane proteins and soluble protein complexes**. *J Biomol NMR* 2014, **59**:1–14.
9. Zumpfe K, Smith AA: **Model-free or not?** *Front Mol Biosci* 2021, **8**.
10. Chevelkov V, Reif B: **TROSY effects in MAS solid-state NMR**. *Concepts Magn Reson A* 2008, **32**(2):143–156.
11. Akke M, Weininger U: **Nmr studies of aromatic ring flips to probe conformational fluctuations in proteins**. *J Phys Chem B* 2023, **127**:591–599.
12. Vugmeyster L: **Recent developments in deuterium solid-state nmr for the detection of slow motions in proteins**. *Solid State Nucl Magn Reson* 2021, **111**, 101710.
13. Tollinger M, Sivertsen AC, Meier BH, Ernst M, Schanda P: **Site-resolved measurement of microsecond-to-millisecond conformational-exchange processes in proteins by solid-state nmr spectroscopy**. *J Am Chem Soc* 2012, **134**:14800–14807.
14. Rovó P, Linser R: **Microsecond timescale protein dynamics: a combined solid-state NMR approach**. *ChemPhysChem* 2018, **19**:34–39.
15. DeAzevedo ER, Hu WG, Bonagamba TJ, Schmidt-Rohr K: **Centerband-only detection of exchange: efficient analysis of dynamics in solids by NMR**. *J Am Chem Soc* 1999, **121**:8411–8412.
16. Krushelnitsky A, DeAzevedo E, Linser R, Reif B, Saalwachter K, Reichert D: **Direct observation of millisecond to second motions in proteins by dipolar CODEX NMR spectroscopy**. *J Am Chem Soc* 2009, **131**:12097–12099.
17. Hologne M, Chen Z, Reif B: **Characterization of dynamic processes using deuterium in uniformly 2H,13C,15N enriched peptides by MAS solid-state NMR**. *J Magn Reson* 2006, **179**:20–28.
18. Lewandowski JR: **Advances in solid-state relaxation methodology for probing site-specific protein dynamics**. *Acc Chem Res* 2013, **46**:2018–2027.
19. Bonaccorsi M, Marchand TL, Pintacuda G: **Protein structural dynamics by magic-angle spinning nmr**. *Curr Opin Struct Biol* 2021, **70**:34–43.
20. ** Marchand TL, Schubeis T, Bonaccorsi M, Paluch P, Lalli D, Pell AJ, Andreas LB, Jaudzems K, Stanek J, Pintacuda G: **1H-Detected biomolecular NMR under fast magic-angle spinning**. *Chem Rev* 2022, **122**:9943–10018.

Outstanding interest: In this review, the concepts behind the recent advancement in sensitivity and resolution of proton-detected solid-state NMR are examined, including ultrafast MAS rates and ultrahigh magnetic fields. Detailed description of the most successful strategies for resonance assignment, structure determination, and dynamics measurement is provided. A number of applications is also reported, ranging from catalysis, through viral infectivity to membrane transport.

21. Krushelnitsky A, Reichert D, Saalwächter K: **Solid-state NMR approaches to internal dynamics of proteins: from picoseconds to microseconds and seconds**. *Acc Chem Res* 2013, **46**:2028–2036.
22. Kurauskas V, Izmailov SA, Rogacheva ON, Hessel A, Ayala I, Woodhouse J, Shilova A, Xue Y, Yuwen T, Coquelle N, *et al.*: **Slow conformational exchange and overall rocking motion in ubiquitin protein crystals**. *Nat Commun* 2017, **8**:1–12.
23. Lewandowski JR, Sass HJ, Grzesiek S, Blackledge M, Emsley L: **Site-specific measurement of slow motions in proteins**. *J Am Chem Soc* 2011, **133**:16762–16765.
24. Lamley JM, Öster C, Stevens RA, Lewandowski JR: **Intermolecular interactions and protein dynamics by solid-state nmr spectroscopy**. *Angew Chem, Int Ed* 2015, **127**:15594–15598.
25. Good D, Pham C, Jagas J, Lewandowski JR, Ladizhansky V: **Solid-state NMR provides evidence for small-amplitude slow domain motions in a multispanning transmembrane α-helical protein**. *J Am Chem Soc* 2017, **139**:9246–9258.
26. Lipari G, Szabo A: **Model-free approach to the interpretation of nuclear magnetic resonance relaxation in macromolecules. 1. theory and range of validity**. *J Am Chem Soc* 1982, **104**:4546–4559.
27. Clore GM, Driscoll PC, Wingfield PT, Gronenborn AM: **Analysis of the backbone dynamics of interleukin-1b using two-dimensional inverse detected heteronuclear 15n-1h nmr spectroscopy**. *Biochemistry* 1990, **29**:7387–7401.
28. Peng JW, Wagner G: **Mapping of spectral density functions using heteronuclear nmr relaxation measurements**. *J Magn Reson* 1992, **98**:308–332.
29. Ishima R, Louis JM, Torchia DA: **Transverse 13c relaxation of chd2 methyl isotopmers to detect slow conformational changes of protein side chains [12]**. *J Am Chem Soc* 1999, **121**:11589–11590.
30. Khan SN, Charlier C, Augustyniak R, Salvi N, Déjean V, Bodenhausen G, Lequin O, Pelupessy P, Ferrage F: **Distribution of pico- and nanosecond motions in disordered proteins from nuclear spin relaxation**. *Biophys J* 2015, **109**:988–999.
31. Smith AA, Ernst M, Meier BH: **Because the light is better here: correlation-time analysis by nmr spectroscopy**. *Angew Chem, Int Ed* 2017, **129**:13778–13783.
32. ** Smith AA, Ernst M, Meier BH: **Optimized "detectors" for dynamics analysis in solid-state nmr**. *J Chem Phys* 2018, **148**, 045104.

Outstanding interest: This paper introduces an optimized framework to characterize motion from solid-state NMR data. The "detectors" estimate the amplitude of motion in a range of correlation times, without defining an explicit motional model. This is necessary due to the inherent ambiguity of relaxation data. The approach is applied to ubiquitin dynamics data, and future integration with MD simulations is proposed.

33. Smith AA: **Interpreting NMR dynamic parameters via the separation of reorientational motion in MD simulation**. *J. Magn. Reson. Open* 2022, **10–11**, 100045.
34. Malär AA, Callon M, Smith AA, Wang S, Lecoq L, Pérez-Segura C, Hadden-Perilla JA, Böckmann A, Meier BH: **Experimental characterization of the hepatitis b virus capsid dynamics by solid-state nmr**. *Front Mol Biosci* 2022, **8**.
35. Chevelkov V, Xue Y, Linser R, Skrynnikov NR, Reif B: **Comparison of solid-state dipolar couplings and solution relaxation**

data provides insight into protein backbone dynamics. *J Am Chem Soc* 2010, **132**:5015–5017.

36. Schanda P, Huber M, Boisbouvier J, Meier BH, Ernst M: **Solid-state NMR measurements of asymmetric dipolar couplings provide insight into protein side-chain motion**. *Angew Chem Int Ed* 2011, **50**:11005–11009.

37. * Gauto DF, Macek P, Malinverni D, Fraga H, Paloni M, Sučec I, Hessel A, Bustamante JP, Barducci A, Schanda P: **Functional control of a 0.5 MDa TET aminopeptidase by a flexible loop revealed by MAS NMR**. *Nat Commun* 2022, **13**:1–13.

Special interest: In this study, the role of a highly flexible loop in the catalytic chamber of the TET2 aminopeptidase is revealed. This region, which was unresolved in the crystallographic structure, is involved in the stabilization of substrate at the catalytic site, as demonstrated by 13CHD2 methyl-directed relaxation dispersion and MD simulations.

38. Schörghuber J, Geist L, Platzer G, Feichtinger M, Bisaccia M, Scheibelberger L, Weber F, Konrat R, Lichtenecker RJ: **Late metabolic precursors for selective aromatic residue labeling**. *J Biomol NMR* 2018, **71**:129–140.

39. Yang CJ, Takeda M, Terauchi T, Jee JG, Kainosho M: **Differential large-amplitude breathing motions in the interface of fkbp12-drug complexes**. *Biochemistry* 2015, **54**:6983–6995.

40. Gauto DF, Macek P, Barducci A, Fraga H, Hessel A, Terauchi T, Gajan D, Miyanoiri Y, Boisbouvier J, Lichtenecker R, Kainosho M, Schanda P: **Aromatic ring dynamics, thermal activation, and transient conformations of a 468 kda enzyme by specific 1h-13c labeling and fast magic-angle spinning nmr**. *J Am Chem Soc* 2019, **141**:11183–11195.

41. Gauto DF, Lebedenko OO, Becker LM, Ayala I, Lichtenecker R, Skrynnikov NR, Schanda P: **Aromatic ring flips in differently packed ubiquitin protein crystals from mas nmr and md**. *J Struct Biol X* 2023, **7**, 100079.

42. Becker LM, Berbon M, Vallet A, Grelard A, Morvan E, Bardiaux B, Lichtenecker R, Ernst M, Loquet A, Schanda P: **The rigid core and flexible surface of amyloid fibrils probed by magic-angle spinning nmr of aromatic residues**. *Angew Chem, Int Ed* 2023, **135**, e202219314.

43. Smith AA, Testori E, Cadalbert R, Meier BH, Ernst M: **Characterization of fibril dynamics on three timescales by solid-state nmr**. *J Biomol NMR* 2016, **65**:171–191.

44. Bonaccorsi M, Knight MJ, Marchand TL, Dannatt HR, Schubeis T, Salmon L, Felli IC, Emsley L, Pierattelli R, Pintacuda G: **Multimodal response to copper binding in superoxide dismutase dynamics**. *J Am Chem Soc* 2020, **142**:19660–19667.

45. Shi C, Öster C, Bohg C, Li L, Lange S, Chevelkov V, Lange A: **Structure and dynamics of the rhomboid protease glpg in liposomes studied by solid-state nmr**. *J Am Chem Soc* 2019, **141**:17314–17321.

46. Rovó P, Smith CA, Gauto D, de Groot BL, Schanda P, Linser R: **Mechanistic insights into microsecond time-scale motion of solid proteins using complementary 15n and 1h relaxation dispersion techniques**. *J Am Chem Soc* 2019, **141**:858–869.

47. * Singh H, Vasa SK, Jangra H, Rovó P, Päslack C, Das CK, Zipse H, Schäfer LV, Linser R: **Fast microsecond dynamics of the protein-water network in the active site of human carbonic anhydrase II studied by solid-state NMR spectroscopy**. *J Am Chem Soc* 2019, **141**:19276–19288.

Special interest: In this study, the elusive dynamics of a functional water–protein network in the active site of hCAII is investigated. Relaxation dispersion data and MD simulations suggest the presence of widespread μs dynamics throughout the catalytic pocket of the enzyme. The presence of an inhibitor, which disrupts the water–protein network, is associated with abrogation of such motion.

48. Rohaim A, Vermeulen BJ, Li J, Kümmerer F, Napoli F, Blachowicz L, Medeiros-Silva J, Roux B, Weingarth M: **A distinct mechanism of c-type inactivation in the kv-like kcsa mutant e71v**. *Nat Commun* 2022, **13**:1–14.

49. Jekhmane S, Medeiros-Silva J, Li J, Kümmerer F, Müller-Hermes C, Baldus M, Roux B, Weingarth M: **Shifts in the selectivity filter dynamics cause modal gating in k+ channels**. *Nat Commun* 2019, **10**:1–12.

50. Marchand TL, Rosa MD, Salvi N, Sala BM, Andreas LB, Barbet-Massin E, Sormanni P, Barbiroli A, Porcari R, Mota CS, Sanctis DD, Bolognesi M, Emsley L, Bellotti V, Blackledge M, Camilloni C, Pintacuda G, Ricagno S: **Conformational dynamics in crystals reveal the molecular bases for d76n beta-2 microglobulin aggregation propensity**. *Nat Commun* 2018, **9**:1–11.

51. Tollinger M, Sivertsen AC, Meier BH, Ernst M, Schanda P: **Site-resolved measurement of microsecond-to-millisecond conformational-exchange processes in proteins by solid-state NMR spectroscopy**. *J Am Chem Soc* 2012, **134**:14800–14807.

52. Kurauskas V, Izmailov SA, Rogacheva ON, Hessel A, Ayala I, Woodhouse J, Shilova A, Xue Y, Yuwen T, Coquelle N, Colletier JP, Skrynnikov NR, Schanda P: **Slow conformational exchange and overall rocking motion in ubiquitin protein crystals**. *Nat Commun* 2017, **8**:1–12.

53. * Zinke M, Sachowsky KA, Öster C, Zinn-Justin S, Ravelli R, Schröder GF, Habeck M, Lange A: **Architecture of the flexible tail tube of bacteriophage spp1**. *Nat Commun* 2020, **11**:1–9.

Special interest: This study demonstrates the potential of combining solid-state NMR data with other structural biology techniques, i.e., cryo-EM. After solving the atomic structure of tail tube of phage SPP1, relaxation measurements and variances in density maps are combined to describe the dynamics of the system. The role of two hinge regions in imparting flexibility to the structure is revealed.

54. Ma P, Xue Y, Coquelle N, Haller JD, Yuwen T, Ayala I, Mikhailovskii O, Willbold D, Colletier J-p, Skrynnikov NR, Schanda P: **Observing the overall rocking motion of a protein in a crystal**. *Nat Commun* 2015, **6**:8361.

55. Krushelnitsky A, Gauto D, Rodriguez DC, Schanda P, Saalwächter K: **Microsecond motions probed by near-rotary-resonance R1ρ 15N MAS NMR experiments : the model case of protein overall-rocking in crystals**. *J Biomol NMR* 2018, **71**:53–67.

56. * Troussicot L, Vallet A, Molin M, Burmann BM, Schanda P: **Disulfide-bond-induced structural frustration and dynamic disorder in a peroxiredoxin from mas nmr**. *J Am Chem Soc* 2023, **145**:10700–10711.

Special interest: In this study, the effect of disulfide-bond formation on the decameric peroxiredoxin Tsa1 is elucidated. Relaxation dispersion data demonstrate the acquisition of μs dynamics of the protein upon oxidaton, in line with the inability to solve the structure of such state by crystallography. Data intepretation was carried out exploiting the recently proposed “detectors” approach.

57. Krushelnitsky A, Hempel G, Jurack H, Ferreira TM: **Rocking motion in solid proteins studied by the ^{15}N proton-decoupled $R_{1\rho}$ relaxometry**. *Phys Chem Chem Phys* 2023, **25**:15885–15896.

58. Ishii Y, Wickramasinghe NP, Chimon S: **A new approach in 1d and 2d 13c high-resolution solid-state nmr spectroscopy of paramagnetic organometallic complexes by very fast magic-angle spinning**. *J Am Chem Soc* 2003, **125**:3438–3439.

59. Linser R, Chevelkov V, Diehl A, Reif B: **Sensitivity enhancement using paramagnetic relaxation in mas solid-state nmr of perdeuterated proteins**. *J Magn Reson* 2007, **189**:209–216.

60. Nadaud PS, Helmus JJ, Sengupta I, Jaroniec CP: **Rapid acquisition of multidimensional solid-state nmr spectra of proteins facilitated by covalently bound paramagnetic tags**. *J Am Chem Soc* 2010, **132**:9561–9563.

61. Öster C, Kosol S, Lewandowski JR: **Quantifying microsecond exchange in large protein complexes with accelerated relaxation dispersion experiments in the solid state**. *Sci Rep* 2019, **9**:1–10.

62. Wang Y, Ribeiro JML, Tiwary P: **Machine learning approaches for analyzing and enhancing molecular dynamics simulations**. *Curr Opin Struct Biol* 2020, **61**:139–145.

63. Noé F, Fabritiis GD, Clementi C: **Machine learning for protein folding and dynamics**. *Curr Opin Struct Biol* 2020, **60**:77–84.

64. Chen H, Chipot C: **Enhancing sampling with free-energy calculations**. *Curr Opin Struct Biol* 2022, **77**, 102497.

65. Bottaro S, Lindorff-Larsen K: **Biophysical experiments and biomolecular simulations: a perfect match?** *Science* 2018, **361**:355–360.